Annals of Biomedical Engineering, Vol. 44, No. 4, April 2016 (© 2015) pp. 1107–1119
DOI: 10.1007/s10439-015-1418-0

In Situ Hydroxyapatite Content Affects the Cell Differentiation on Porous Chitosan/Hydroxyapatite Scaffolds

ANAMARIJA ROGINA,[1] PATRICIA RICO,[2,3] GLORIA GALLEGO FERRER,[2,3] MARICA IVANKOVIĆ,[1] and HRVOJE IVANKOVIĆ[1]

[1]Faculty of Chemical Engineering and Technology, University of Zagreb, Marulićev trg 19, p.p.177, 10001 Zagreb, Croatia; [2]Center for Biomaterials and Tissue Engineering (CBIT), Universitat Politècnica de València, Camino de Vera s/n, 46022 Valencia, Spain; and [3]Biomedical Research Networking Center in Bioengineering, Biomaterials and Nanomedicine (CIBER-BBN), Zaragoza, Spain

(*Received 16 June 2015; accepted 4 August 2015; published online 12 August 2015*)

Associate Editor Jane Grande-Allen oversaw the review of this article.

Abstract—Highly porous chitosan/hydroxyapatite composite structures with different weight ratios (100/0; 90/10; 80/20; 70/30; 60/40; 50/50; 40/60) have been prepared by precipitation method and freeze-gelation technique using calcite, urea phosphate and chitosan as starting materials. The composition of prepared composite scaffolds was characterized by X-ray diffraction analysis and Fourier transformed infrared spectroscopy, while morphology of scaffolds was imaged by scanning electron microscopy. Mercury intrusion porosimetry measurements of prepared scaffolds have shown different porosity and microstructure regarding to the HA content, along with SEM observations of scaffolds after being immersed in physiological medium. The results of swelling capacity and compressive strength measured in Dulbecco's phosphate buffer saline (DPBS) have shown higher values for composite scaffolds with lower *in situ* HA content. Viability, proliferation and differentiation of MC3T3-E1 cells seeded on different scaffolds have been evaluated by live dead assay and confocal scan microscopy. Our results suggest that the increase of HA content enhance osteoblast differentiation confirming osteogenic properties of highly porous CS/HA scaffolds for tissue engineering applications in bone repair.

Keywords—Chitosan, Hydroxyapatite, Scaffold, Unconfined compression, Porosity, MC3T3-E1 differentiation, Osteogenic markers.

Address correspondence to Anamarija Rogina, Faculty of Chemical Engineering and Technology, University of Zagreb, Marulićev trg 19, p.p.177, 10001 Zagreb, Croatia. Electronic mail: arogina@fkit.hr, parico@upvnet.upv.es, ggallego@ter.upv.es, mivank@fkit.hr, hivan@fkit.hr

INTRODUCTION

In recent years, there are numerous investigations regarding the synthesis of new biodegradable scaffolds for bone tissue replacement. To fulfill required features of potential biomaterial substituent, wide range of synthetic and natural polymers along with calcium phosphate phases were used. The main goal is to produce a material that will mimic extracellular matrix (ECM) of bone. Synthetic polymers are generally inert to biological molecules; therefore, natural polymers are more adequate for these purposes. Chitosan (CS) has shown to be a good candidate for tissue engineering materials due to its chemical similarity to biological molecules and short-time biodegradability *in vivo via* specific enzymatic reactions.[17,18] Apart from chemical structure, chitosan can be processed by different techniques for scaffold production: lyophilization, electrospinning, thermally induced phase separation (TIPS), particulate leaching, microsphere sintering, etc.[7,16,24,33,34]

The potential material for tissue engineering (TE) applications has to fulfill several requirements, such as biocompatibility, bioactivity, biodegradability and good mechanical properties. However, scaffold's topography (surface roughness), charge and wettability, microstructure and interconnected porosity are the main factors influencing the cell adhesion and activity, neovascularization and angiogenesis.[4,5,11,20] Besides surface properties, the alteration of scaffold's composition during neotissue formation affects further cell proliferation and growth. Calcium phosphate salts have shown good resorption ability in physiological conditions, and depending on its composition, higher

solubility.[3,6,21] For instance, octacalcium phosphate (OCP) has tendency to transform to calcium-deficient hydroxyapatite (CDHA) similar to biological apatite by hydrolysis reaction. By transforming, OCP influences the adsorption of specific biomolecules important for cell activation.[30,31] Even though stoichiometric hydroxyapatite is the most studied bioactive component of bone tissue engineering (BTE) scaffolds, *in situ* precipitation of CDHA or carbonated HA (CHA) will allow producing biomaterials more similar to the inorganic part of natural bone tissue.

Natural bone can be defined as a metabolically active tissue that undergoes continuous remodeling process involving bone formation and bone resorption. These counteracting processes are based on activity of osteoblasts (bone formation), osteoclasts (bone resorption) and osteocytes (bone maintenance). Under normal conditions, kinetics of bone resorption and bone formation are balanced, i.e., the amount of removed bone is always equal to the amount of newly formed bone tissue.[9,25] In terms of fracture, bone tissue healing is initiated in response to regulatory mechanisms associated with inflammation and immune response. Bone repair process involves several stages that cause interactions between various types of tissue: endochondral formation (cartilage formation), intramembranous bone formation, followed by primary bone formation due to cartilage resorption, and finally bone remodeling process.[8] New bone synthesis is controlled within osteoblasts and progenitor cells through signaling mechanisms that regulate the actions and transcription levels of various transcription factors. Those transcription factors are involved in the regulation of the osteoblast phenotype, which in turn regulate genes that code for bone matrix proteins.[12] Runt-related transcription factor 2 (Runx2) is considered to be a central control gene within the osteoblast's phenotype which supports final progression to the mature osteocyte and expression of obligatory genes for mineralization of the bone extracellular matrix. Runx2 is principally linked to osteoblast proliferation and differentiation, which is indicated by increment of its expression during osteoblast maturation. The Runx2 transcript possesses ability to stimulate genes such as: osteocalcin, osteopontin, collagen I, collagenase 3 (matrix metalloproteinase 1), bone sialoprotein, alkaline phosphatase etc., which are considered to reflect different aspects of osteoblast function and of bone formation.[12,25,28]

This work is a continuation of our previous studies[23] of the effect of *in situ* formed HA in chitosan solution on the properties of highly porous CS/HA composite scaffolds prepared by freeze-gelation technique. Different amount *in situ* non-stoichiometric HA has shown significant influence on scaffolds microstructure, while MTS assay confirmed no toxic effect on fibroblast L929 cells evaluated by indirect viability tests. In this work, osteogenic properties of highly porous CS/HA scaffolds were evaluated by *in vitro* culture of preosteoblast MC3T3-E1 cells during 14 days under optimal differentiation conditions. Live dead assay was performed to evaluate cell viability, while expression of specific osteogenic differentiation markers was evaluated by immunocitochemical assays on cells seeded onto different CS/HA scaffolds compositions.

MATERIALS AND METHODS

Synthesis and Characterization

Scaffold's Preparation

Composite scaffolds were prepared by freeze-gelation technique. Prior to highly porous structure formation, chitosan ($\bar{M}$ = 100–300 kg mol^{-1}, deacetylation degree, DD = 0.95–0.98; Acros Organics) was dissolved in aqueous 0.36% acetic acid (HAc) solution to form 1.2 wt% polymer solution. To synthesize HA, an appropriate amount of calcite ($CaCO_3$) and urea phosphate ($(NH_2)_2CO$–H_3PO_4) in a Ca/P ratio of 1.67 was added into CS solution. The starting content of these reagents were scaled according to the final CS/HA theoretical weight ratios of 100/0, 90/10, 80/20, 70/30, 60/40, 50/50 and 40/60. Obtained solutions/suspensions were set in molds and cooled down to 4 °C before being frozen at −22 °C for 18 h. Then, frozen samples were immersed into neutralization medium of 1 mol dm^{-3} NaOH/ethanol (1:1) at −22 °C for 12 h to induce gelation of chitosan. The wet samples were removed from solution and rinsed in ethanol at −22 °C for 12 h, then at room temperature for 24 h, and finally dried at room temperature. Highly porous scaffolds (HPS) were produced and designated as follows: HPS-0, HPS-1, HPS-2, HPS-3, HPS-4, HPS-5 and HPS-6, corresponding to chitosan/hydroxyapatite weight ratio of 100/0; 90/10; 80/20; 70/30; 60/40; 50/50 and 40/60, respectively.

Scaffold's Characterization

The Fourier transform infrared spectra (FTIR) of scaffolds were recorded by attenuated total reflectance (ATR) spectrometer for solids with a diamond crystal (Bruker Vertex 70) at 20 °C over the spectral range of 4000–400 cm^{-1}, with 16 scans and 4 cm^{-1} of resolution.

Mineralogical composition of prepared scaffolds was investigated by X-ray diffraction analysis (XRD) using a Shimadzu XRD-6000 diffractometer with Cu Kα radiation operated at 40 kV and 30 mA, in the

range of $5° < 2\theta < 70°$ at a scan speed of 0.2°/s. Identification of crystal phases was done by ICDD (International Centre for Diffraction Data) card catalog.

Morphology of highly porous scaffolds was imaged by the scanning electron microscope TESCAN Vega3SEM Easyprobe at electron beam energy of 10 keV. Previously to imaging, scaffolds were frozen for cutting to preserve the porous microstructure. Cutted samples were sputtered with gold for 120 s.

Pore size distribution was determined by means of a mercury porosimeter from Micromeritics (Autopore IV (9500)), as a function of intrusion volume (pressure) of mercury. Due to the high porosity of the samples, the weight of analyzed samples ranged from 20 to 30 mg per scaffold.

Physical Properties

Swelling Ability

The swelling capacity of each composite scaffold ($n = 3$) was measured in Dulbecco's phosphate buffer saline (DPBS) at 37 °C for 24 h. For greater standardization of weight measurement, wet samples taken out from DPBS were exposed for 5 min to ambient temperature and atmospheric pressure. The weights of the wet scaffolds were then determined, denoted as w_1. Afterwards, samples were vacuum dried at 50 °C until constant mass and weighted again. The weights of the dry scaffolds were denoted as w_2. Swelling capacity was calculated as the ratio of increased weight after immersion ($w_1 - w_2$) relative to weight w_2.

Mechanical Tests

Unconfined compression of scaffolds was performed in DPBS at room temperature. Prior to measurement, each composite scaffold ($n = 5$) was immersed in DPBS for 24 h to reach swelling equilibrium. Unconfined compression was performed on swollen cylindrical scaffolds, 8 mm in diameter, with mechanical instrument Seiko TMA/SS6000 (Seiko Instrument Inc., Japan) in three steps: (1) a pre-deformation from 0 to 2% of sample height at a rate of 200 μm/min to normalize an initial reference test point, (2) an intermediate step where this deformation was maintained for 2 min, and (3) a final step from 2 to 80% deformation at a rate of 50 μm min^{-1}.

Biological Evaluation

Argon plasma Treatment

Cell culture with MC3T3-E1 preosteoblasts was performed on HPS-0, HPS-1, HPS-3 and HPS-5 to investigate the influence of scaffolds composition on cell adhesion, proliferation and differentiation. Prior to cell culture, scaffolds were treated with argon plasma surface modification performed in order to increase cell adhesion.[27] Argon plasma treatment was carried out on Plasma Electronic Piccolo, 2.45 GHz generator, with argon pressure of 50 Pa for 120 s on both sides of scaffolds. Then, treated samples were swollen in DPBS for 24 h and cut into cylindrical shape with diameter of 6 mm and 1–2 mm of height.

Cell Culture on Scaffolds

Cell culture with mouse MC3T3-E1 cell line was performed on plasma treated scaffolds for 1, 7 and 14 days. Plasma treated cylindrical-shaped replicas ($n = 3$) were sterilized with 70% ethanol in vacuum and conserved at 4 °C for 24 h. After sterilization, samples were washed 3 times in DPBS and left immersed for 30 min. Final washing was performed with Dulbecco's modified Eagle's culture medium (DMEM) and replicas were transported into a 96-well plate previously coated with agar. Agar was deposited in polystyrene plates in order to avoid cell adhesion onto wells and to favor confinement of cells inside scaffolds in early adhesion stages.

Meanwhile, MC3T3-E1 cells were maintained in basal medium with 10% FBS until they achieve confluence. Scaffolds were seeded with 2.7×10^5 cells/scaffold and incubated with DMEM medium supplemented with 10% FBS (fetal bovine serum) and 1% penicillin/streptomycin in humidified atmosphere with 5% CO_2 at 37 °C. After 3 days of culture, medium was changed to differentiation medium composed of DMEM supplemented with 10% FBS, 1% penicillin/streptomycin, 50 μg/ml ascorbic acid, 10 mM β-glycerophosphate and 1 μM dexamethasone. Medium was changed every third day.

Live Dead Assay

Qualitative cell viability on cultured composite scaffolds at 1, 7 and 14 days was determined with live/dead staining by Live/Dead® Viability/Cytotoxicity Kit (Invitrogen). Cultured samples were washed 3 times with DPBS and incubated with 2 μM calcein acetoxymethyl (calcein-AM) and 4 μM ethidium homodimer (EthD-1) in humidified atmosphere with 5% CO_2 at 37 °C for 15 min. Live cells (stained in green) and dead cells (stained in red) were analyzed by fluorescence microscope (Leica TCS SP2 AOBS, Leica Microsystems).

Cell Counting

Cell proliferation on different composite scaffolds at 1, 7 and 14 days was estimated by cell nucleus counting using DAPI staining on different scaffold slices with

60 μm of thickness cutted in a Leica CM1520 cryotome at −20°C. Imaging was carried out by confocal fluorescence microscope (Zeiss LSM 780, Axio Observer) in 16-tile mode scanning. Prior to statistical calculation, outlier samples were discarded. Cell number on different scaffolds is expressed as mean ± SEM (standard error of mean) to indicate the precision of estimated mean of population.

Immuno Assay

Differentiation of MC3T3-E1 preosteoblasts at 1, 7 and 14 days was examined by different antibodies to confirm expression of differentiation markers: runt-related transcription factor 2 (Runx2), osteopontin (OPN) and integrin-binding sialoprotein (IBSP). Firstly, cultured samples were washed with DPBS and permeabilized with DPBS/Triton X-100 0.5% for 5 min at room temperature, and subsequently blocked by DPBS/5% goat serum for 1 h. Then incubation with primary antibodies with dilution 1:100 in DPBS/5% goat serum was performed for 2 h at room temperature. Next, samples were washed with DPBS/0.5% Tween 20 and incubated with secondary Cy3 conjugated anti-rabbit and anti-mouse antibodies with dilution 1:200 for 2 h at room temperature, with subsequent addition of 5 μL of phallacidin per scaffold for cytoskeleton staining. After washing second antibodies, samples were conserved in 30% sucrose solution for 24 h at 4 °C and finally fixed with cryoprotective medium (OCT) at -80°C. Sample slices with 60 μm of thickness were cut in a Leica CM1520 cryotome at −20 °C and mounted with Vectashield® DAPI for nuclei staining. Detection of protein markers was performed by confocal fluorescence microscope (Zeiss LSM 780, Axio Observer).

Statistical Analysis

The results are expressed as mean ± standard deviation (SD) or as mean ± SEM (standard error of mean). Statistical comparisons between samples were examined using one-way ANOVA analysis with value $p < 0.05$ or $p < 0.01$ as a statistical significance.

RESULTS

In FTIR spectra (Fig. 1, left) characteristic phosphate (PO_4^{3-}) bands at two wave number regions are seen: 1022–960 and 600–560 cm^{-1}. All prepared scaffolds (except HPS-1) show absorption band at 875 cm^{-1} which could be associated with HPO_4^{2-} or CO_3^{2-} group. The presence of apatite structure substitutions indicates a non-stoichiometric HA formation with higher solubility in physiological conditions, regarding the stoichiometric HA. Characteristic chitosan bands, amid I and II (–NHC=O) and amino ($–NH_2$), are depicted in Fig. 1, left and Table 1. Amid I (carbonyl part) and amino bands are clearly present in all samples accompanied with slight shift regarding to the pure chitosan scaffold (HPS-0).

X-ray diffraction analysis of composite scaffolds confirmed apatite phase formation (Fig. 1, right). Composite scaffolds with lower HA portion (HPS-2) show presence of other calcium phosphate phase, octacalcium phosphate (OCP), while HPS-1 scaffold shows characteristic maximum of chitosan anhydrous polymorph phase (CPA), as well.

SEM imaging shows highly porous structure of HPS-0, HPS-1, HPS-3 and HPS-5 scaffolds after being immersed in DPBS and vacuum dried at 50 °C (Fig. 2). Drastic changes in pore size and shape with higher HA content are noted. In addition, good pore interconnectivity of scaffolds is present.

The analysis of swelling properties of different composite scaffolds has indicated the highest swelling capacity of HPS-1 (23.3 ± 0.1), while the lowest value of 13.6 ± 0.6 has HPS-6 scaffold (Fig. 3). The significant decrease of swelling ability regarding the chitosan scaffold happens at HA portions higher than 30%. Young's moduli measured in wet conditions (DPBS) have similar behavior as swelling capacity, i.e., HPS-1 scaffold possesses the highest compressive strength with modulus value of 6.63 ± 0.73 kPa, which decreases by the HA addition.

Open porosity values obtained by mercury intrusion porosimetry are in range 84–91% for all prepared scaffolds (except HPS-5: 73.0%). Each scaffold has a wide distribution of pore diameter (Fig. 4), where HPS-4 scaffold excels with highest maximum of pore diameter distribution (d_{50} = 76.5 μm), which could be a reason for having the lowest Young's modulus.

Cell culture with MC3T3-E1 preosteoblast cells was performed on HPS-0, HPS-1, HPS-3 and HPS-5 scaffolds for 1, 7 and 14 day. Cell viability was evaluated by live dead staining, in which live cells are stained in green and dead cells appear in red. Green staining of cells on investigated scaffolds (Supplementary data 1, Fig. SD1) confirms good cell viability. Nuclei counting method have confirmed effective cell seeding into the scaffolds and the increment of the cell number along the time on each scaffold (Fig. 5). The decrement in cell number after 14 days of culture suggests that cells have been stopped proliferating and started to differentiate, which has been indicated by immunological assay presented in following results. Although HPS-5 shows lower cell number, the tendency of cell proliferation is the same compared with other composite scaffolds, which confirms good behavior for cell pen-

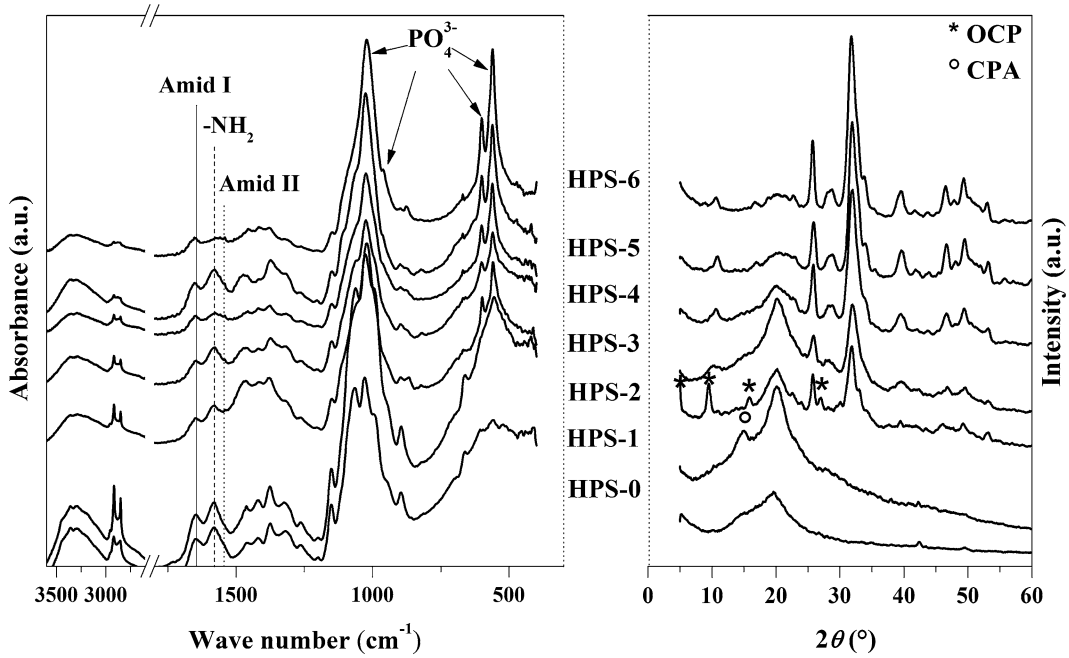

FIGURE 1. FTIR spectra (left) and XRD pattern (right) of prepared composite scaffolds.

TABLE 1. FTIR bands (*k*) of amid I (–C=O), amino (–NH_2) and amid II (–NH–) bond of composite scaffolds.

Scaffold	*k* (amid I) (cm^{-1})	*k* (amino) (cm^{-1})	*k* (amid II) (cm^{-1})
HPS-0	1651	1589	1562
HPS-1	1650	1581	1562
HPS-2	1648	1579	1560
HPS-3	1647	1577	1560
HPS-4	1650	1577	1558
HPS-5	1652	1579	1560
HPS-6	1652	1575	1558

etration, adhesion and growth. The addition of HA to the chitosan matrix favors cell colonization, as the number of cells in the composites is higher than in the pure chitosan scaffold for all culture times.

Immunological assays of cell differentiation confirmed by bone formation markers are depicted in Figs. 5, 6, 7, and 8 (and in Supplementary data 2–4). Cell nuclei appeared in blue, cytoskeletons in green and specific proteins expression in red, respectively.

Runt-related transcription factor 2 (Runx2) as an early-stage osteoblast differentiation marker has been detected in cells seeded on HPS-3 and HPS-5 scaffold at day 1 (Fig. 6) and day 7, while expression in scaffolds HPS-0 and HPS-1 is absent during the entire period of culture (Supplementary data, Figs. SD2a and SD2b). The Runx2 has the ability to facilitate the convergence of osteogenic signaling pathways, therefore, expression of osteopontin (OPN) and integrin binding sialoprotein (IBSP) is expected. The expression of OPN and IBSP has been found in HPS-3 and HPS-5 scaffolds at 1, 7 and 14 days of culture (Figs. 6, 7) suggesting good osteogenic potential of the scaffolds. On contrary, HPS-0 and HPS-1 have showed only OPN expression at day 7 and 14 (Supplementary data 3–4).

DISCUSSION

Scaffold's Characterization

The results of FTIR spectra of HPS composite scaffolds show phosphate groups characteristic for apatite phase (Fig. 1).[1,26] Results of our previous study[22] have indicated possible interactions between *in situ* formed HA and chitosan. In FTIR spectra of CS/HA composites the phosphate band shifting was observed, regarding the phosphate band of pure hydroxyapatite prepared at the same conditions. According to the literature[15] the protonated amino

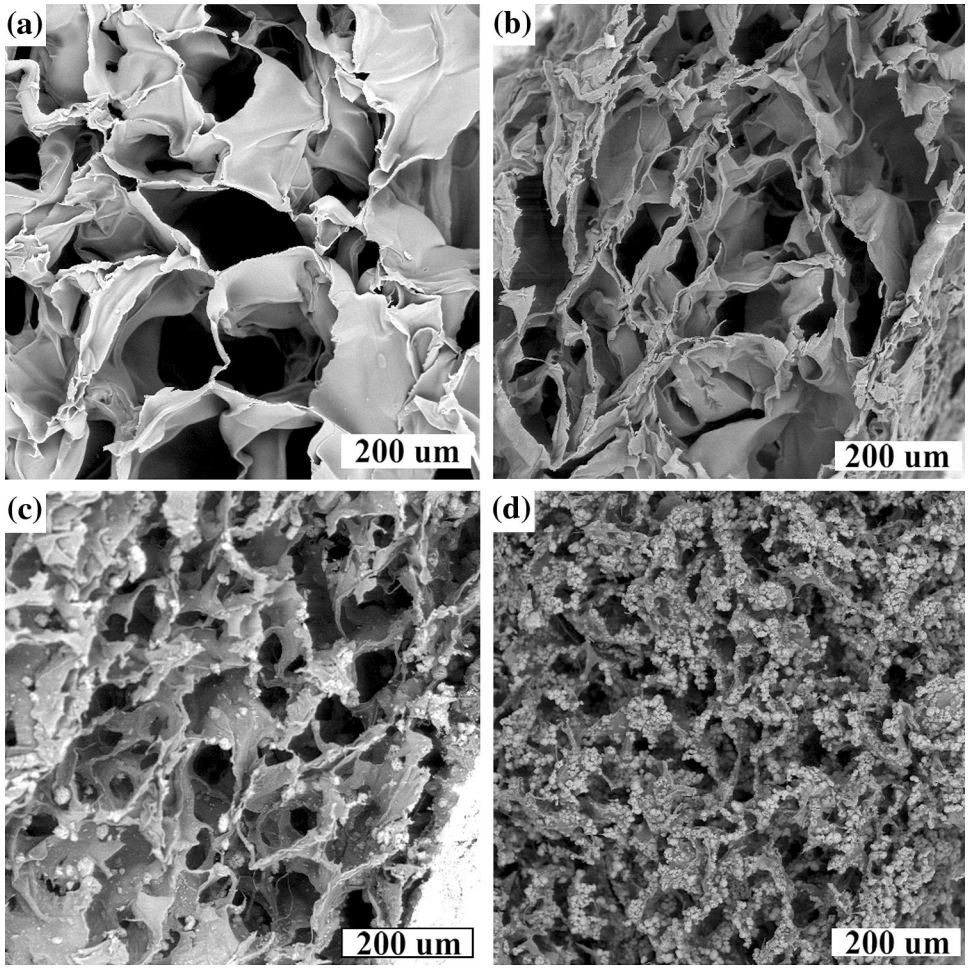

FIGURE 2. SEM micrographs of cross section of (a) HPS-0; (b) HPS-1; (c) HPS-3; (d) HPS-5 scaffold after 24 h of DPBS immersion.

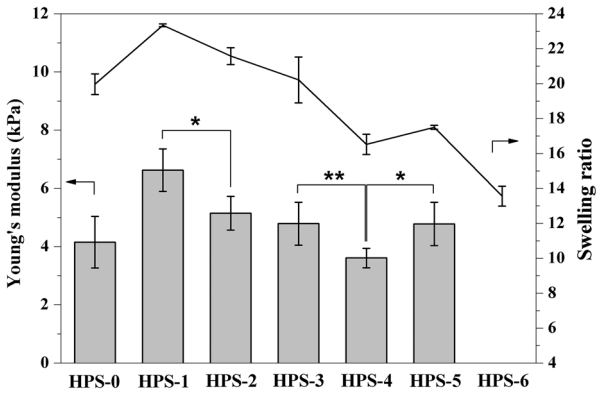

FIGURE 3. Swelling ratio (line) and Young's modulus (bars) of porous scaffolds after 24 h of DPBS immersion at 37 °C (significant difference between two groups: *$p < 0.05$, **$p < 0.01$).

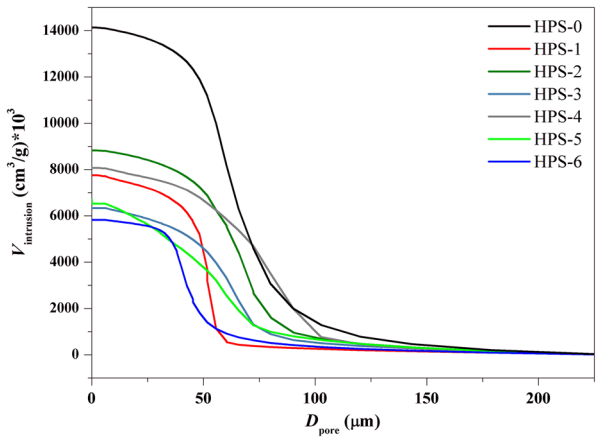

FIGURE 4. Mercury intrusion volume vs. pore size (D_p) of composite scaffolds.

groups of chitosan, NH_3^+, being positively charged form complex with phosphate ions facilitating nucleation and growth of HA. The carbonyls of chitosan can chelate calcium ions and arrange them into a similar structure as HA crystal. In present study, the shifts of specific chitosan groups (amid I and amino) in composite scaffolds (Table 1) could indicate possible chitosan–HA interactions.

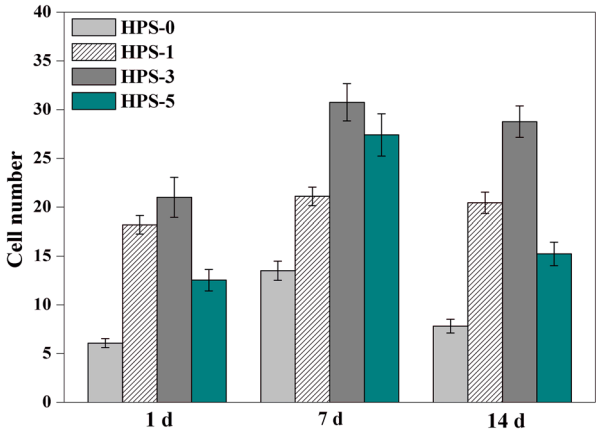

FIGURE 5. Cell proliferation on different composite scaffolds at 1, 7 and 14 days of culture.

Confirmation of HA precipitation has obtained by X-ray mineralogical analysis, according to ICDD data base. Besides characteristic HA diffraction maxima, another calcium phosphate phase has been identified as octacalcium hydrogen phosphate pentahydrate (OCP). Coexistence of hydroxyapatite and OCP has been found in scaffold HPS-2, which is not surprising regarding the suggested transformation mechanism of OCP to HA *via* hydrolysis reaction in slightly acidic conditions.[10,29] The presence of OCP does not interfere with bioactivity or biocompatibility of scaffolds. Moreover, conversion of OCP in physiological conditions leads to calcium-deficient hydroxyapatite (CDHA) similar to biological apatite. Those OCP-HA transformation reactions are also implicated in adsorption of serum and glycoproteins, i.e., in cell activity. The existence of chitosan anhydrous polymorph (CSA) is caused by the preparation method which uses a mixture of ethanol and NaOH as a gelling medium.[14,23]

Swelling, Mechanical Properties and Porosity

One of the main factors that influence the biocompatible nature of artificial biomaterials is swelling property, i.e., content of absorbed water which imparts physicochemical properties to biomaterial. It is well known that chitosan swells in aqueous solution, which could be utilized as a biomaterial protection inside the implanted space.[19] All prepared scaffolds show high swelling ratio (>130%) after 24 h being immersed in DPBS at 37 °C (Fig. 3), which is of great importance for cells and nutrients diffusion, and prevention of the body fluid loss. The swelling ratio values indicate that scaffolds have capacity to uptake and retain water content greater than their own weight which is advantage in practical applications to have stable implant during cell culture or implanted site contact. Higher content of inorganic phase (HPS-4, HPS-5 and HPS-6) influences the absorbed water amount causing constraining the swelling. This effect can be described as a formation of HA barrier that prevents water permeation into chitosan matrix. On the other hand, scaffolds with lower inorganic phase content (HPS-1and HPS-2) show slight increase in swelling capacity regarding the pure chitosan scaffold. The inorganic HA phase within chitosan matrix acts also as a filler that could improve physicochemical properties of the material, depending on the fraction added to the matrix. Lower HA precursor's amount can allow precipitation of smaller crystals of inorganic phase homogeneously dispersed. That way, better matrix-filler interactions and lower interface energy without forming agglomerates, that represent weak load-bearing point of the material, are obtained. Moreover, during the swelling, texture of scaffolds is changing from soft sponge to hydrocolloid by the increment of absorbed water. With additional affect of ionic strength of testing medium, it seems that lower content of inorganic phase influences the formation of 3D stable structure.

Unconfined compression has been measured for swollen scaffolds from HPS-0 to HPS-5. The absence of Young's modulus of HPS-6 scaffold is due to its high brittleness and inability to perform compressive testing. Deformation of each composite scaffold under compressive loading follows the same trend (Supplementary data 5, Fig. SD5). When compressive loading is applied, scaffolds show elastic behavior due to chitosan ability to form a hydrogel. Likewise, spongy structure is responsible for inability to determine the maximum loading at break. HPS-1 scaffold shows significant difference in Young's modulus with respect to pure chitosan scaffold (HPS-0). As seen from Fig. 3 the lower content of inorganic phase results in better mechanical properties, as shown by Young's modulus. It is believed that the interaction between HA and chitosan (ionic and/or polar) assist the site specific nucleation and growth of HA nano-particles and enable more stress to be transferred from the matrix to the filler during external loading.[15] High amounts of nano-sized filler can result in agglomeration of the particles that represent weak load-bearing point of the composite material. Interesting question arises by correlating water uptake ability and mechanical properties of composite scaffolds that are following the same fashion. The highest swelling capacity and Young's modulus has obtained for HPS-1 scaffold, which could imply the synergistic effect of water uptake on mechanical properties of swollen scaffold. However, composite scaffolds with higher HA content (HPS-4 and HPS-5) possess ability to uptake a signif-

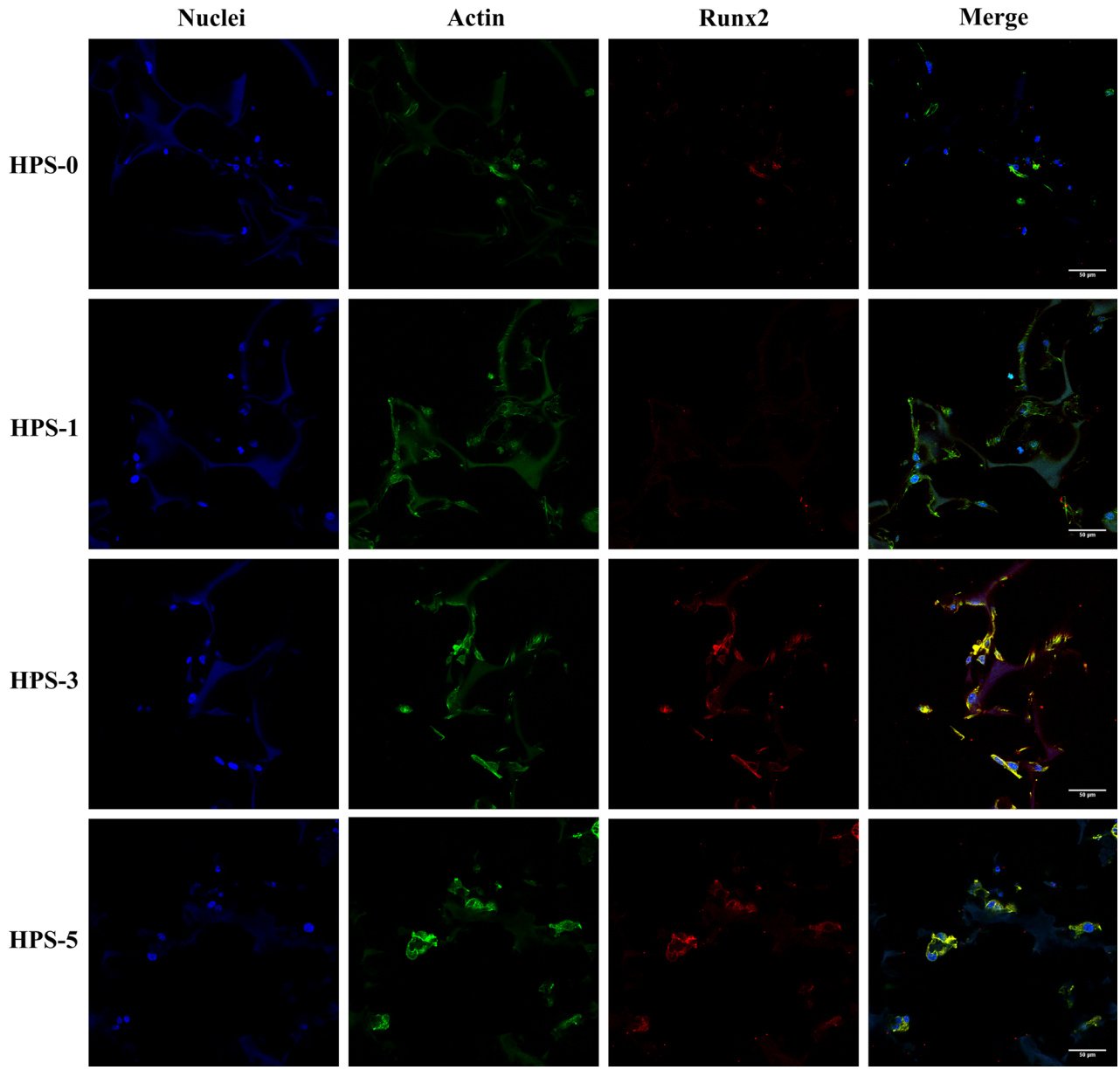

FIGURE 6. Expression of Runx2 on different composite scaffolds after 1 day of culture. Cells nuclei detected with Dapi (blue), cytoskeleton with phallacidin (green), Runx2 (red). Scale bar: 50 μm.

icantly lower amount of water compare to the pure chitosan scaffold, still significant difference in Young's modulus regarding the chitosan has not been emphasized. It can be assumed that water uptake ability implicates mechanical properties of swollen scaffolds, since the amount of absorbed water depends not only on materials composition, yet on the difference in porosity and pore size distribution of the scaffold.[32] Those properties complicate the understanding of the impact of HA content on compressive strength of investigated composite scaffolds.

Referring the mercury intrusion porosimetry results (Fig. 4), the slight difference in pore size distribution between composite scaffolds can be noticed (except HPS-5 scaffold). Even though HPS-0 and HPS-2 scaffolds possess similar pore size distribution, HPS-2 shows significantly greater water uptake. This could imply the isolated influence of HA as a reinforcement agent during the material swelling, and indirect reinforcement under compressive load. Higher impact of pore size distribution on compressive modulus could be assigned to HPS-4 scaffold, as a composite scaffold with largest pores and the most unstable swollen structure.

Correlating the pore size and porosity, mineralogical composition and crystallinity, microstructure of

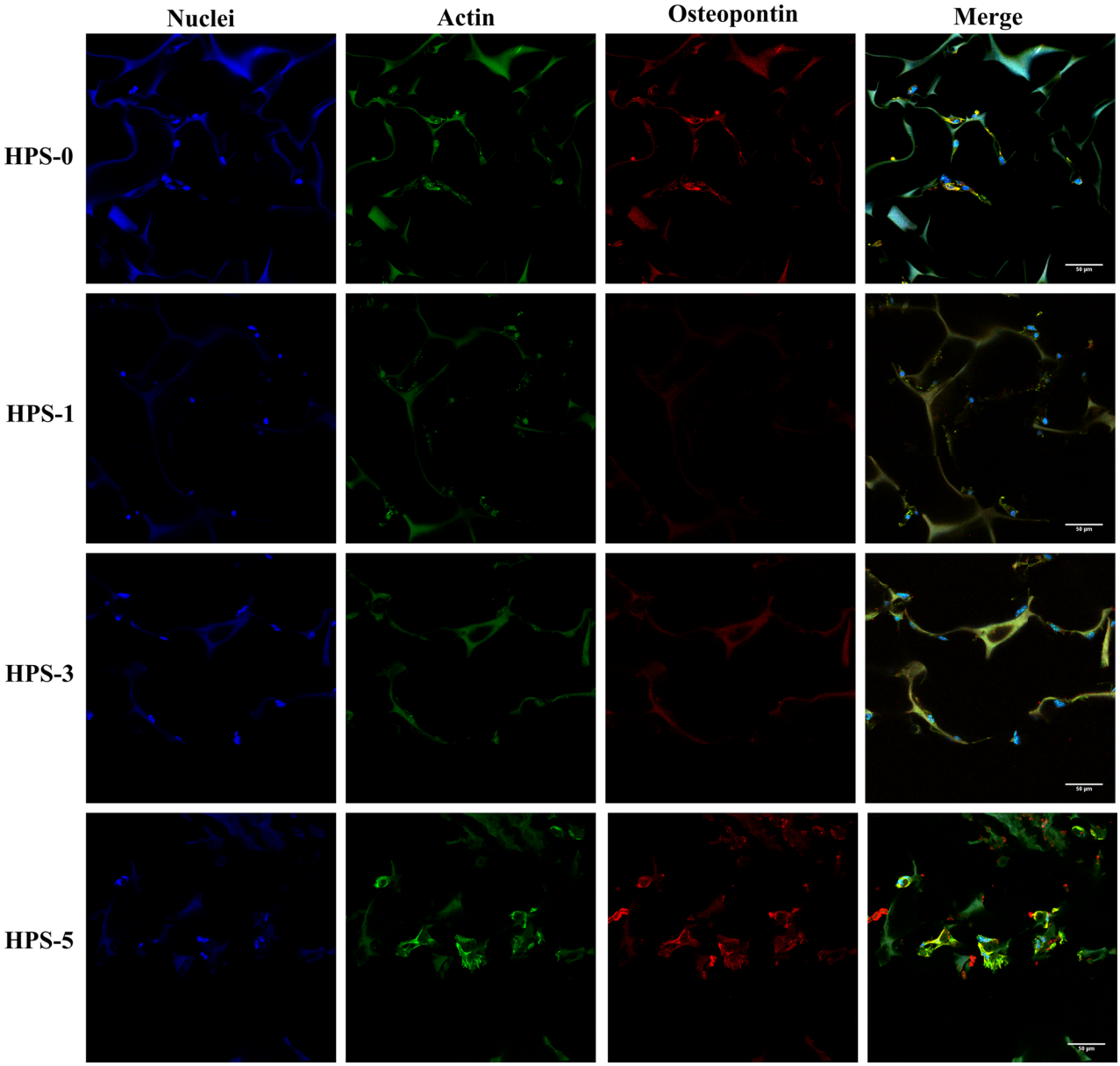

FIGURE 7. Expression of OPN on different composite scaffolds after 14 days of culture. Cells nuclei detected with Dapi (blue), cytoskeleton with phallacidin (green), osteopontin (red). Scale bar: 50 μm.

scaffolds, and regarding the wet conditions of testing (swelling ability); it is hard to isolate the influence of inorganic phase content on porous scaffolds compressive strength. Even though swollen HPS-1 composite scaffold in phosphate buffer saline possesses higher Young's modulus than chitosan scaffold, its application as a bone substituent is limited on bone defect repair. Therefore, future work will be focused on modifying mechanical properties of composite scaffolds introducing another synthetic polymer to extend material's application.

Comparing the pore size distribution results obtained by mercury intrusion porosimetry (MIP) with the visual assessment by SEM imaging, broad distribution of pore size of scaffolds is observed. MIP calculation is based on hypothesis of material having cylindrical pores, and regarding to the non-defined porous structure of composite scaffolds (Fig. 2), it can be assumed the existence of pore sizes larger than ~100 μm. So far, different pore size and structure has been suggested for regeneration of various tissues.[13] Pore sizes of 100–400 and 200–350 μm have been suggested for tissue regeneration and osteoconduction, while pore sizes of 5–15 and 70–120 μm could be optimal for fibroblast and chondrocytes growth. It is clear that optimal design for scaffold's microstructure

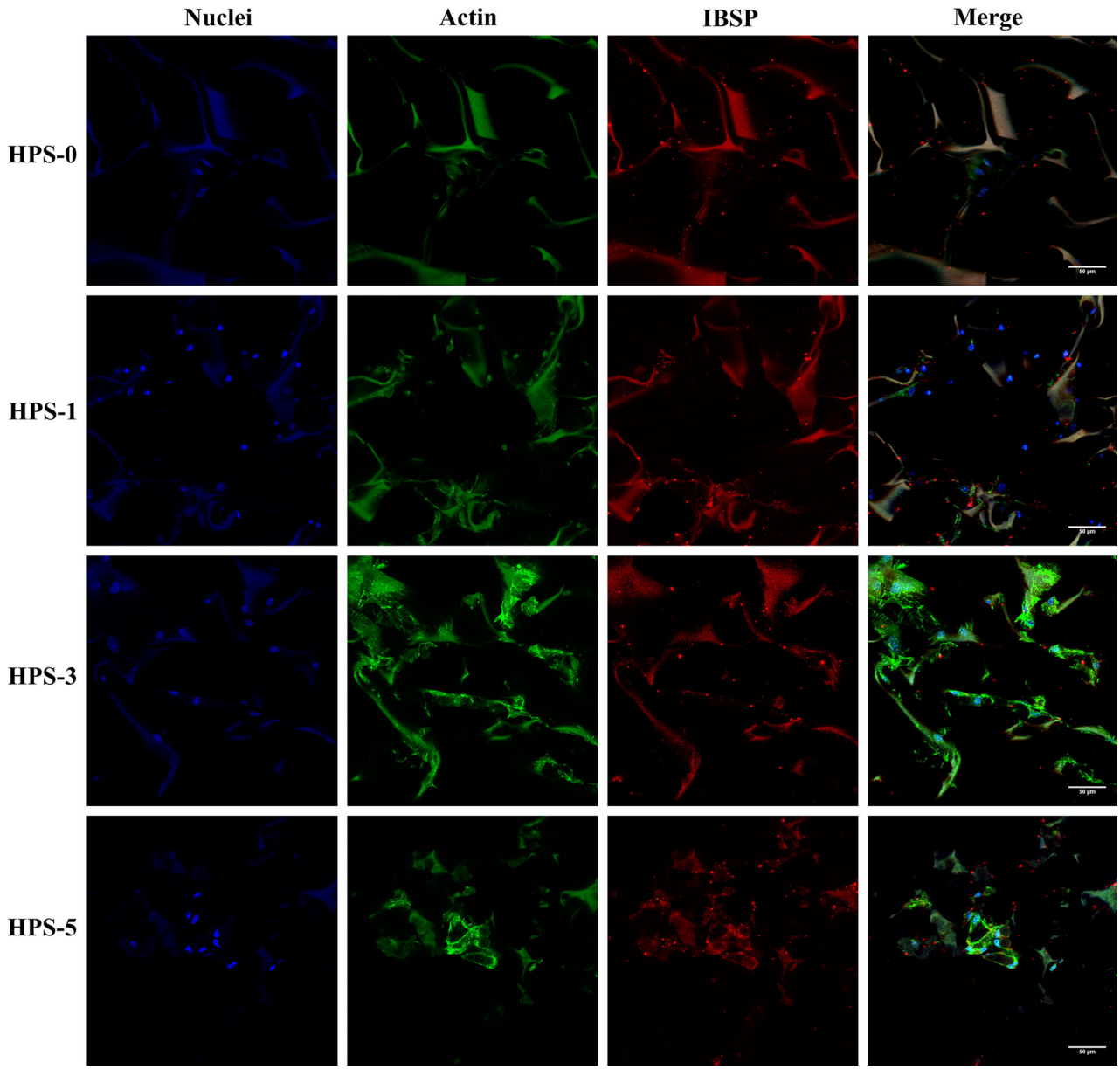

FIGURE 8. Expression of IBSP on different composite scaffolds after 14 days of culture. Cells nuclei detected with Dapi (blue), cytoskeleton with phallacidin (green), IBSP (red). Scale bar: 50 μm.

and pore size distribution depends on the cell type which will be applied.

Live Dead Assay and Cell Proliferation

Fluorescence staining of HPS-0, HPS-1 HPS-3 and HPS-5 scaffolds shows good cell viability during the whole period of culture (Supplementary data, Fig. SD1). It can be noticed the homogeneous cell distribution through the scaffold's trabeculae, and cell number seems to increase over culture time. Beside good cell distribution, the cell orientation around HA particles on scaffolds HPS-3 and HPS-5 can be observed. Cell adhesion and proliferation depends on surface properties of the scaffolds, such as hydrophilicity, electrostatic charge, roughness, etc. It is a fact that synthetic polymers are mostly hydrophobic in their unmodified state which influences the cellular proliferation. Cell adhesion to an artificial material is provided by molecules of extracellular matrix adsorbed from culture media or deposited by the cells themselves.[2] Chitosan is a natural hydrophilic polymer that contains specific amino groups possibly responsible for preferable adsorption of binding molecules (proteins). The presence of HA has positive influence on the cell number which could be a result of synergic effect of

hydrophilicity and bioactivity. In addition to the effects of surface wettability and polarity the scaffold surface topography, i.e., surface roughness obtained by the plasma treatment may also affect protein adhesion and consequently cellular responses.

Cell proliferation obtained by nuclei counting has confirmed positive indication of live dead assay by good cell adhesion and growth on each investigated scaffold. Significant cell proliferation points out high surface area of all composite scaffolds and sufficiently large porosity and pore sizes for cell penetration and proliferation. As mentioned above, primary cell adhesion stage depends on surface properties and material's composition, but also on porosity, interconnectivity and pore size. A close look on porosity values of composite scaffolds (84–91%) revels slight difference which can be eliminated as a determination factor for cell proliferation in HPS-0, HPS-1 and HPS-3 scaffolds. Therefore, it can be concluded that increment in cell number in scaffolds with HA content is a results of bioactive component presence. Lower cell number in HPS-5 scaffolds at primary cell adhesion stage could indicate the effect of lower porosity, yet it is not unique important factor affecting cell adhesion and growth. Regarding the cell number calculated from pure chitosan scaffold, positive influence of hydroxyapatite in cell adhesion and proliferation as a bioactive component can be confirmed.

Qualitative Protein Expression

Immunological assays were performed on HPS-0, HPS-1, HPS-3 and HPS-5 scaffolds at 1, 7 and 14 days of culture. Expression of specific markers, as osteoblast phenotypes, was used to confirm MC3T3-E1 preosteoblast cell differentiation.

When implanted in an osseous site, bone bioactive materials such as calcium phosphate implants and coatings provide a suitable environment for cellular response and osteoblasts colonization. The addition of calcium phosphate, mainly hydroxyapatite, in chitosan scaffold has shown to increase cell adhesion, proliferation, alkaline phosphatase activity, protein adsorption, Type 1 collagen production and expression of other osteogenic differentiation markers. Runx2 as a principal osteogenic master gene for bone formation that switches bone development and osteoblast differentiation has been detected on scaffolds with higher HA content (HPS-3 and HPS-5). Runx2 promotes genes essential for progression of differentiation at early stages of osteoblast differentiation and during the extracellular matrix mineralization process. Detection of principal osteogenic marker on HPS-3 and HPS-5 scaffolds at day 1 and 7 is accompanied by expression of non-collagenous proteins osteopontin and integrin-binding sialoprotein during the whole period of culture. The lack of Runx2 expression in HPS-0 and HPS-1 scaffolds for each time point of culture indicates poor osteogenic signal of those scaffolds. On the basis of detection of osteogenic markers expression, it can be concluded that chitosan/HA porous scaffolds with higher content of *in situ* HA would provide suitable environment for enhanced osteogenesis of MC3T3-E1 preosteoblasts. Additional quantitative analysis of proteins quantity would give detailed information regarding the correlation of HA content in porous composite scaffold with cell differentiation mechanism.

CONCLUSIONS

Highly porous chitosan/HA scaffolds were prepared by precipitation reactions and freeze-gelation method. Different portions of hydroxyapatite have impact on physical and biological properties of composite scaffolds. Compressive strength and swelling capacity measured in physiological conditions have shown that critical HA portion which improves chitosan properties do not exceeds 30 wt%. Cell culture experiment confirmed cell viability of preosteoblast MC3T3-E1 cells during 14 days of culture. Qualitative analysis of osteoblast's phenotype expression indicates cell differentiation on chitosan/HA scaffolds with higher HA content. According to the positive osteogenic signal with higher *in situ* HA content and interconnected microstructure, presented scaffolds have shown to be a potential candidate for repair of bone tissue defects.

ELECTRONIC SUPPLEMENTARY MATERIAL

The online version of this article (doi:10.1007/s10439-015-1418-0) contains supplementary material, which is available to authorized users.

ACKNOWLEDGMENT

The financial support of the Croatian Science Foundation (project: "Development of Biocompatible Hydroxyapatite Based Materials for Bone Tissue Engineering Applications") and L'Oréal-UNESCO Foundation 'For Women in Science' is gratefully acknowledged. The financial support from the Spanish Ministry of Economy and Competitiveness and the Feder funds through the MAT2013-46467-C4-1-R project is acknowledged by the Spanish co-authors. CIBER-BBN is an initiative funded by the VI National R&D&I Plan 2008-2011, Iniciativa Ingenio 2010, Consolider Program. CIBER Actions are financed by

the Instituto de Salud Carlos III with assistance from the European Regional Development Fund. The authors want to acknowledge Pilar Gómez Tena and Sergio Mestre Beltrán from Instituto de Tecnología Cerámica, Castellon, Spain, for theirs assistance with porosity measurements.

REFERENCES

[1]Azzaoui, K., A. Lamhamdi, E. M. Mejdoubi, M. Berrabah, B. Hammouti, A. Elidrissi, M. M. G. Fouda, and S. S. Al-Deyab. Synthesis and characterization of composite based on cellulose acetate and hydroxyapatite application to the absorption of harmful substances. *Carbohydr. Polym.* 111:41–46, 2014.

[2]Bacakova, L., E. Filova, M. Parizek, T. Ruml, and V. Svorcik. Modulation of cell adhesion, proliferation and differentiation on materials designed for body implants. *Biotech. Adv.* 29:739–767, 2011.

[3]Bose, S., and S. Tarafder. Calcium phosphate ceramic systems in growth factor and drug delivery for bone tissue engineering: a review. *Acta Biomater.* 8:1401–1421, 2012.

[4]Chan, B. P., and K. W. Leong. Scaffolding in tissue engineering: general approaches and tissue-specific considerations. *Eur. Spine J.* 17:467–479, 2008.

[5]Dhandayuthapani, B., Y. Yoshida, T. Maekawa, and D. S. Kumar. Polymeric scaffolds in tissue engineering application: a review. *Int. J. Polym. Sci.* 1–19:2011, 2011.

[6]Dorozhkin, S. V. Calcium orthophosphate-based bioceramics. *Materials* 6:3840–3942, 2013.

[7]Frohbergh, M. E., A. Katsman, G. P. Botta, P. Lazarovici, C. L. Schauer, U. G. K. Wegst, and P. I. Lelkes. Electrospun hydroxyapatite-containing chitosan nanofibers crosslinked with genipin for bone tissue engineering. *Biomaterials* 33:9167–9178, 2012.

[8]Gerstenfeld, L. C., C. M. Edgar, S. Kakar, K. A. Jacobsen, and T. A. Einhorn. Osteogenic growth factors and cytokines and their role in bone repair. In: Engineering of Functional Skeletal Tissues, in Topics in Bone Biology, edited by M. C. Farach-Carson, A. G. Mikos, and F. Bronner. London: Springer, 2005, pp. 17–44.

[9]Harada, S.-I., and G. A. Rodan. Control of osteoblast function and regulation of bone mass. *Nature* 423:349–355, 2003.

[10]Ishihara, S., T. Matsumoto, T. Onoki, T. Sohmura, and A. Nakahira. New concept bioceramics composed of octacalcium phosphate (OCP) and dicarboxylic acid-intercalated OCP *via* hydrothermal hot-pressing. *Mater. Sci. Eng. C* 29:1885–1888, 2009.

[11]Karageorgiou, V., and D. Kaplan. Porosity of 3D biomaterial scaffolds and osteogenesis. *Biomaterials* 26:5474–5491, 2005.

[12]Kirkham, G.R., Cartmell, S.H. Genes and proteins involved in the regulation of osteogenesis. In: Topics in Tissue Engineering, edited by N. Ashammakhi, R.L. Reis, and E. Chiellini, R.R.E.C., 2007. pp. 1–22.

[13]Lee, H., and G. H. Kim. Cryogenically fabricated three-dimensional chitosan scaffolds with pore size-controlled structures for biomedical applications. *Carbohydr. Polym.* 85:817–823, 2010.

[14]Lewandowska, K. Miscibility and interactions in chitosan acetate/poly(Nvinylpyrrolidone) blends. *Thermochim. Acta* 517:90–97, 2011.

[15]Li, J., D. Zhu, J. Yin, Y. Liu, F. Yao, and K. Yao. Formation of nano-hydroxyapatite cristal in situ in chitosan-pectin polyelectrolyte complex network. *Mater. Sci. Eng. C* 30:795–803, 2010.

[16]Martel-Estrada, S. A., C. A. Martínez-Pérez, J. G. Chacón-Nava, P. E. García-Casillas, and I. Olivas-Armendariz. Synthesis and thermo-physical properties of chitosan/poly(dl-lactide-co-glycolide) composites prepared by thermally induced phase separation. *Carbohydr. Polym.* 81:775–783, 2010.

[17]Martins, A. M., R. C. Pereira, I. B. Leonor, H. S. Azevedo, and R. L. Reis. Chitosan scaffolds incorporating lysozyme into CaP coatings produced by a biomimetic route: a novel concept for tissue engineering combining a self-regulated degradation system with in situ pore formation. *Acta Biomater.* 5:3328–3336, 2009.

[18]Martins, A. M., M. I. Santos, H. S. Azevedo, P. B. Malafaya, and R. L. Reis. Natural origin scaffolds with in situ pore forming capability for bone tissue engineering applications. *Acta Biomater.* 5:1637–1645, 2008.

[19]Mohamed, K. R., Z. M. El-Rashidy, and A. A. Salama. *In vitro* properties of nanohydroxyapatite/chitosan biocomposites. *Ceram. Int.* 37:3265–3271, 2011.

[20]O'Brien, F. J. Biomaterials & scaffolds for tissue engineering. *Mater. Today* 14:88–95, 2011.

[21]Osborn, J. F., and H. Newesely. The material science of calcium phosphate ceramics. *Biomaterials* 1:108–111, 1980.

[22]Rogina, A., M. Ivanković, and H. Ivanković. Preparation and characterization of nano-hydroxyapatite within chitosan matrix. *Mater. Sci. Eng. C* 33:4539–4544, 2013.

[23]Rogina, A., P. Rico, G. Gallego Ferrer, M. Ivanković, and H. Ivanković. Effect of in situ formed hydroxyapatite on microstructure of freeze-gelled chitosan-based biocomposite scaffolds. *Eur. Polym. J.* 68:278–287, 2015.

[24]Sarem, M., F. Moztarzadeh, and M. Mozafari. How can genipin assist gelatin/carbohydrate chitosan scaffolds to act as replacements of load-bearing soft tissues? *Carbohydr. Polym.* 93:635–643, 2013.

[25]Seibel, M. J. Biochemical markers of bone turnover part I: biochemistry and variability. *Clin. Biochem. Rev* 26:97–122, 2005.

[26]Shaltout, A. A., M. A. Allam, and M. A. Moharram. FTIR spectroscopic, thermal and XRD characterization of hydroxyapatite from new natural sources. *Spectrochim. Acta A* 83:56–60, 2011.

[27]Silva, S. S., S. M. Luna, M. E. Gomes, J. Benesch, I. Paskuleva, J. F. Mano, and R. L. Reis. Plasma surface modification of chitosan membranes: characterization and preliminary cell response studies. *Macromol. Biosci.* 8:568–576, 2007.

[28]Stein, G. S., J. B. Lian, A. J. van Wijnen, J. L. Stein, M. Montecino, A. Javed, A. K. Zaidi, D. W. Young, J.-Y. Choi, and S. M. Pockwinse. Runx2 control of organization, assembly and activity of the regulatory machinery for skeletal gene expression. *Oncogene* 23:4315–4329, 2004.

[29]Suvorova, E. I., F. Christensson, H. E. Lundager Madsen, and A. A. Chernov. Terrestrial and space-grown HAP and OCP crystals: effect of growth conditions on perfection and morphology. *J. Cryst. Growth* 186:262–274, 1998.

[30]Suzuki, O. Interface of synthetic inorganic biomaterials and bone regeneration. *Int. Congr. Ser.* 1284:274–283, 2005.

[31]Suzuki, O., S. Kamakura, T. Katagiri, M. Nakamura, B. Zhao, Y. Honda, and R. Kamijo. Bone formation enhanced by implanted octacalcium phosphate involving conversion into Ca-deficient hydroxyapatite. *Biomaterials* 27:2671–2681, 2006.

[32]Wagoner Johnson, A. J., and B. A. Herschler. A review of the mechanical behavior of CaP and CaP/polymer composites for applications in bone replacement and repair. *Acta Biomater*. 7:16–30, 2011.

[33]Wang, Y.-C., M.-C. Lin, D.-M. Wang, and H.-J. Hsieh. Fabrication of a novel porous PGA-chitosan hybrid matrix for tissue engineering. *Biomaterials* 24:1047–1057, 2003.

[34]Yuan, N. Y., Y. A. Lin, M. H. Ho, D. M. Wang, J. Y. Lai, and H. J. Hsieh. Effect of the cooling mode on the structure and strength of porous scaffolds made of chitosan, alginate and carboxymethyl cellulose by freeze-gelation method. *Carbohydr. Polym*. 78:349–356, 2009.